# Experimental study on lattice-shaped cement treatment method for liquefaction countermeasure

## Étude expérimentale d'un procédé d'anti-liquéfaction des sols au moyen d'un bâti en forme de treillage en béton

Takahashi H., Morikawa Y.
*Port and Airport Research Institute, Yokosuka, Japan*

Iba H.
*Toa Corporation, Yokohama, Japan*

Fukada H.
*Fudo Tetra Corporation, Tokyo, Japan*

Maruyama K., Takehana K.
*Geodesign Corporation, Tokyo, Japan*

ABSTRACT: In the present study, a new method to improve sandy ground is proposed as a liquefaction countermeasure. It is the floating-type and lattice-shaped cement treatment method, where cement treated soil is not fixed to an unliquefiable stratum. However, a fixed-type structure such as treated soil should be formed at the side of the floating-type treated soil to reduce its lateral displacement. In the study, one-dimensional dynamic response analyses were firstly conducted to confirm the mechanism of the new method. Secondly, a series of centrifuge model tests were performed to demonstrate the effect in a proto-type scale's stress condition. The analyses and model tests confirmed the effect of liquefaction countermeasure of the new method.

RÉSUMÉ : Dans la présente étude, nous proposons une nouvelle méthode de consolidation en terrain sableux comme une mesure pour contrer la liquéfaction du sol. C'est une méthode qui consiste à traiter le sol au moyen d'un bâti en forme de treillage en béton de type flottant: le terrain ainsi consolidé par le béton n'est pas amarré à une strate non liquéfiable. Cependant, afin de réduire son déplacement latéral, il faudra construire à l'endroit du sol de type flottant traité une structure de type fixe. Dans notre étude, nous avons mené en premier lieu des analyses de la réponse dynamique à une dimension pour vérifier le fonctionnement de ce nouveau procédé. Deuxièmement, nous avons réalisé une série de tests sur modèles centrifugés afin de montrer l'effet de la méthode mise en œuvre lors de secousses provoquées sur des modèles réduits. Les analyses et les tests sur modèles centrifugés qui ont été menés ont confirmé l'efficacité du nouveau procédé.

KEYWORDS: lattice shape, cement treatment, liquefaction countermeasure

## 1 INTRODUCTION

Liquefaction induced by earthquake generates sand boiling and ground settlement. Other problems were also reported, including the decrease of bearing capacity and the increase of horizontal earthpressure against retaining walls. To prevent those problems caused by liquefaction of ground, various countermeasure methods have been proposed, such as the cement deep mixing and the high-pressure jet mixing methods. Those methods have a big advantage of being able to be applied for ground that contains fine-grain fraction soil. Furthermore, the controversial displacement caused by the construction can be reduced. In Japan, a lattice-shaped cement treatment method has been frequently used for many construction sites to prevent liquefaction, where cement-treated piles are intersected to form the lattice as shown in Fig. 1. The lattice-shaped walls can reduce shear stress generated by earthquake in liquefiable sandy ground, restricting the liquefaction there. Meanwhile, the construction cost of the cement treatment is relatively higher than other methods, such as the Sand Compaction Pile (SCP) method, and expected to be cut down. Especialy, the cost of the high-pressure jet mixing method, which can be applied for the liquefiable ground under exsiting structures, is significantly high. Therefore, decreasing total volume of cement treatment is required with the aim of reducing the construction cost.

In the present paper, the new method as shown in Fig. 2 is proposed as a liquefaction countermeasure in which the lattice-shaped treatment soil is not fixed to an unliquefiable stratum below a liquefiable layer, namely a floating-type improvement method. The fixed-type structure such as cement treated soil should be formed at the side of the floating-type treated soil to reduce its lateral displacement. It can synchronize the lateral motions of the floating-type treated soil and unliquefiable stratum, and reduce shear stress of an in-between stratum, preventing the liquefaction.

In the study, one-dimensional dynamic response analyses were firstly conducted to verify the mechanism of the new method. Secondly, a series of centrifuge model tests were

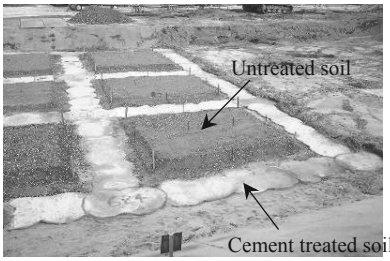


Figure 1. Surface of ground improved by lattice-shaped cement treatment method

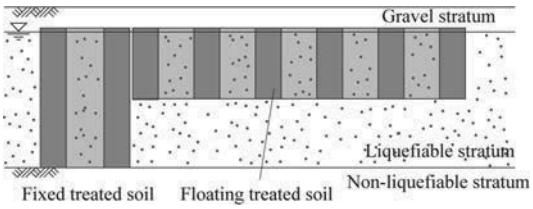


Figure 2. Schematic view of floating-type and lattice-shaped treatment method

performed to demonstrate the effect in a stress condition

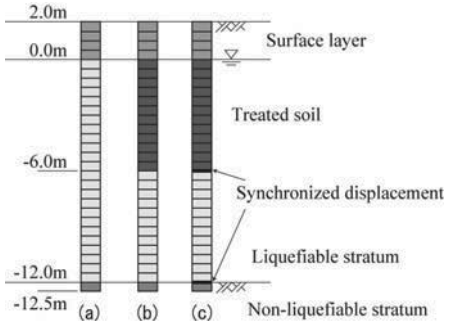


Figure 3. 1D numerical model to verify the mechanism of floating-type method

Table 1. Soil parameters for numerical analyses

| | $G_0$(MN/m$^2$) ($\sigma_0$'=98kN/m$^2$) | $\rho$ (g/cm$^3$) | $\phi$ (deg.) | $h_{max}$ |
|---|---|---|---|---|
| Surface layer | 62 | 1.84 | 39.0 | 0.24 |
| Treated soil | 150 | 2.04 | - | - |
| Liquefiable layer | 62 | 2.04 | 39.0 | 0.24 |
| Non-liquefiable layer | 37 | 2.04 | - | - |

corresponding to a proto-type scale. There were two series of model tests, which were called Series A and B. In Series A, rigid side-walls of a specimen box were used to reduce the lateral displacement of the floating-type treated soil. Meanwhile, a fixed-type structure was placed at the side of the floating-type treated soil in Series B. Through these series, the effect of countermeasure was examined.

## 2 VERIFICATION OF MECHANISM

One-dimensional dynamic response analyses besed on a finite element method were used to assess the amplitude of shear stress of the stratum between the floating-type treated soil and unliquefiable stratum. Figure 3 shows the analytical model, and Table 1 is the list of soil parameters for the anayses. Case a was for unimproved ground, and Cases b and c were for improved ground. The lateral motions of the floating-type treated soil and unliquefiable stratum were synchronized in Case c, not in Case b. An elasto-plastic hyperbolic model was used for surface and liquefiable layers as constitutive relations, and a linear elastic model was for cement treated soil and unliquefiable layer. Generation of excess pore water pressure was not modeled, because the analyses were mainly conducted to verify low shear stress of unimproved ground. The sinusoidal waves were input for the numerical models, and its maximum amplitude and shaking period were 3.0 m/s$^2$ and 20 seconds, respectively.

Figure 4 shows the depth distribution of maximum shear strain calculated. As shown in Fig. 4, the shear strain at the deeper stratum in Case b as well as Case a significantly increased. With the large shear strain being generated, the deeper stratum will be liquefied. In contrast, the shear strain at the deeper stratum in Case c remained small due to the synchronism of the motions of floating-type treated soil and unliquefiable stratum. Thus, the synchronism of floating-type treated soil and unliquefiable stratum takes effect, restricting shear stress and liquefaction of in-between unimproved stratum.

## 3 CENTRIFUGE MODEL TESTS

### 3.1 *Test model and procedures*

Figure 5 shows cross-section views of models in Series A and B, and Table 2 is the list of test cases. As for the width of floating-type treated soil, it was shortened because of the limitation of width of specimen box used. Series A used the specimen box with the height of 20.0 m, the width of 28.0 m, and the depth of 9.0 m, although these values are converted to proto-type scales.

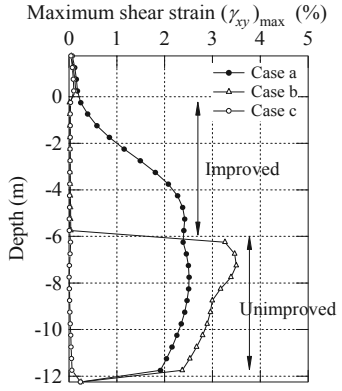


Figure 4. Shear strain distribution

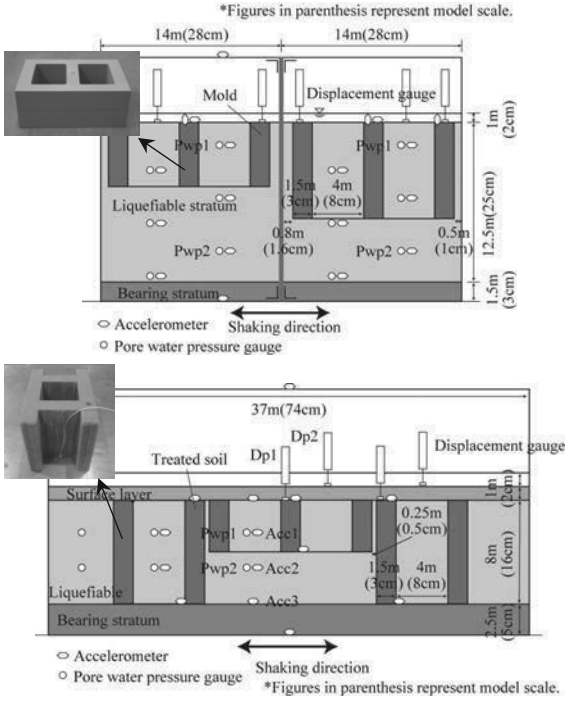


Figure 5. Cross-section view of model grounds: upper; Series A, lower; Series B

Meanwhile, Series B used the specimen box with the height of 25.0 m, the width of 37.0 m, and the depth of 10.0 m.

Firstly, a uniform unliquefiable sandy layer was prepared by the technique of sand raining. Secondly, accelerometers and pore water pressure gauges were hanged at their spots, followed by another sand raining for liquefiable sandy layer. The sand material was the cat.5 of Sohma sand that was taken in Japan. Thirdly, the sand raining was stopped at the depth of the bottom surface of floating-type treated soil, and the flat surface of sand layer was formed by a vacuum. Finally, the model of floating-type treated soil was put on the surface and filled with liquefiable sand. The average relative densities of liquefiable stratum were $D_r$ = 46 ~ 54 % in Series A and $D_r$ = 48 ~ 57 % in Series B, respectively. In Series B, a surface layer was made to model subgrade bed, using special cat.4 of Sohma sand. This layer did not liquefy due to the high permeability.

The model of lattice-shaped treated soil in Series A was a polyvinyl chloride mold, the unit weight of which was 13.7 kN/m$^3$. In Series B, the cement treated soil of cat. 5 of Sohma sand was used as the mold. It was made by mixing with sand and early-strength cement at the dry weight ratio of 20 %. The unconfined compressive strength of cement treated soil was 3219 ~ 5300 kN/m$^2$, and the wet unit weight was 18.0 ~ 19.8 kN/m$^3$. The grid spacing of lattice-shaped treated soil was set as 4 m. This spacing was based on the test result our previous work (Takahashi *et al.*, 2006a, 2006c).

Table 2. List of model test cases

| Series | Case | Type | Depth of treated soil | | |
|---|---|---|---|---|---|
| | | | Left | Center | Right |
| A | A1 | Unimproved | - | 0.0 m | - |
| | A2 | Floating-type | - | 5.0 m | - |
| | A3 | Floating-type | - | 7.5 m | - |
| | A4 | Floating-type | - | 10.0 m | - |
| | A5 | Fixed-type | - | 12.5 m | - |
| B | B1 | Unimproved | 0.0 m | 0.0 m | 0.0 m |
| | B2 | Fixed-type | 8.0 m | 8.0 m | 8.0 m |
| | B3 | Floating-type | 8.0 m | 4.0 m | 8.0 m |
| | B4 | Floating-type | 8.0 m | 6.0 m | 8.0 m |
| | B5 | Floating-type | 0.0 m | 4.0 m | 8.0 m |
| | B6 | Floating-type | 8.0 m | 2.0 m | 8.0 m |

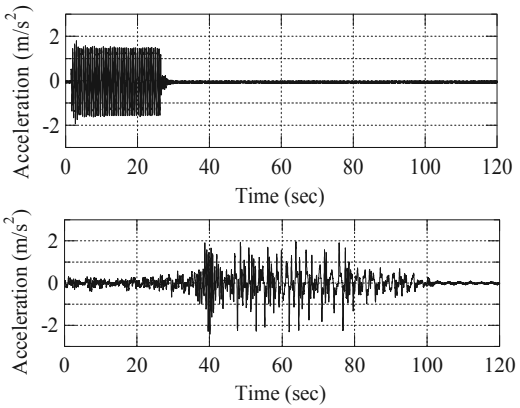


Figure 6. Measured acceleration of ground: upper; Series A (A1&A4), lower; Series B (B1)

Fluid, which was made 50 times viscous by methylcellulose, was used as pore water to fit time scaling between dynamic behaviour and dissipation of excess pore water pressure in a centrifuge. In Series A, $CO_2$ gas was percolated and deaired, followed by the percolation of viscous fluid in a gravitational field. In Series B, viscous fluid was percolated into the model ground in a centrifuge without $CO_2$ and deairing. This percolation method was proposed by Okamura & Inoue (2012), and it could make sandy ground saturated by reducing unsaturated zone during percolation with the help of the centrifugal acceleration.

After preparing tested model, shaking tests were conducted by using the centrifuge facility Mark II owned by the Port and Airport Research Institute. The details of the facility can be seen in the report by Kitazume & Miyajima (1995). Moreover, the validity of a dynamic centrifuge model test on ground liquefaction inside grids was shown by Takahashi *et al*. (2006b, 2006c). In these reports, the modelling of models method was used to assess the validity of a centrifuge test.

In Series A, the input signal for shaking was 50 sine waves, which had the frequency of 100 Hz. 100 Hz corresponds to 2 Hz in a proto-type scale. In the meanwhile, the input signal of Series B was irregular wave simulating huge Level-2 earthquake. In both series, the acceleration level was increased stepwise, keeping the wave shape. Response acceleration, excess pore water pressure, and settlement of model ground were measured during the shaking. The examples of response acceleration measured at the bottom of the specimen box in Cases A1, A4, and B1 are shown in Fig. 6.

### 3.2 *Test results of Series A*

This section discussed the test results of Series A. Figure 7 shows the relationship between the input acceleration and the maximum value of excess pore water pressure, $(\Delta u/\sigma')_{max}$, in a proto-type scale. As $\Delta u/\sigma'$ fluctuated during the shaking, the middle value of fluctuating $\Delta u/\sigma'$ is chosen as $(\Delta u/\sigma')_{max}$.

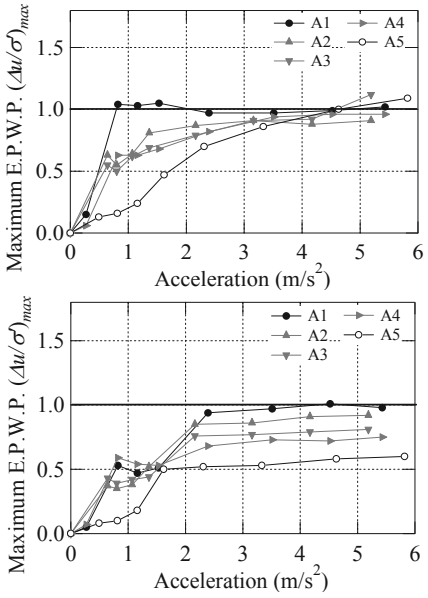


Figure 7. Maximum excess pore water pressure: upper; depth of 2.6 m at Pwp1, lower; depth of 10.0 m at Pwp2

Figures 8(a) and (b) represent the values at the depth of 2.6 m (Pwp1 in Fig. 5) and 10.0 m (Pwp2 in Fig. 5), respectively.

As shown in Fig. 7(a), $(\Delta u/\sigma')_{max}$ of A1 increased to 1.0 even below the input acceleration level of 1.0 m/s$^2$. This means that a shallow layer in unimproved ground such as Case A1 could easily liquefy by a relatively weak earthquake. On the other hand, $(\Delta u/\sigma')_{max}$ of A2 ~ A4, in which only the shallow layer was improved, were below 0.7, and thus the floating-type improvement took effect in the shallow layer. $(\Delta u/\sigma')_{max}$ of A5 was at a lower level of 0.2, and the effect of the ground improvement was the largest in A2 ~ A5. Additionally, the acceleration level when $(\Delta u/\sigma')_{max}$ was 1.0 was over 4.0 m/s$^2$ in A2 ~A4, and this level was corresponding to the level of A5.

In Fig. 7(b), $(\Delta u/\sigma')_{max}$ of A1 and A2 ~ A4 did not have a clear difference below the input acceleration level of 2.0 m/s$^2$, but those differed above the level of 2.0 m/s$^2$. To be more specific, $(\Delta u/\sigma')_{max}$ of A1 remained stable around 1.0 above the input of 2.0 m/s$^2$, and those of A2 ~ A4 did around 0.7 ~ 0.9. The deeper improvement made $(\Delta u/\sigma')_{max}$ lower. $(\Delta u/\sigma')_{max}$ of A5 stayed constant around 0.5 ~ 0.6. According to these results, the floating-type improvement took effect, restricting excess pore water pressure at both shallow and deep layers. In addition, the improvement effect became larger by deepening the improvement depth of the floating-type treated soil.

### 3.3 *Test results of Series B*

#### 3.3.1 *Properties of pore water pressure*

This sub-section discussed the properties of pore water pressure measured. Time histories of excess pore water pressure ratio, $\Delta u/\sigma'$, are shown in Fig. 8 in a proto-type scale. Each figure shows the ratios at the depth of 3.5 m (Pwp1 in Fig. 5) and 7.0 m (Pwp2 in Fig. 5) in B1, B2, and B4. The input acceleration level was around 1.97 m/s$^2$.

As shown in Fig. 8(a), $\Delta u/\sigma'$ at the depth of 3.5 m in B1, the unimprovement case, sharply increased to 1.0, and the ground was liquefied shortly after subjected to the principal motion. Furthermore, $\Delta u/\sigma'$ slowly decreased after the principal motion, and this meant that the ground was fully liquefied. $\Delta u/\sigma'$ at the depth of 7.0 m also increased to 1.0 by the principal motion and slowly decreased after that. These properties indicated that the ground was liquefied throughout the liquefiable layer.

On the other hand, $\Delta u/\sigma'$ in B2, the fixed-type improvement case, did not reach 1.0, but approached 0.9 by the principal motion. It should be noted that $\Delta u/\sigma'$ promptly decreased after

the principal motion. This behaviour indicated that the ground

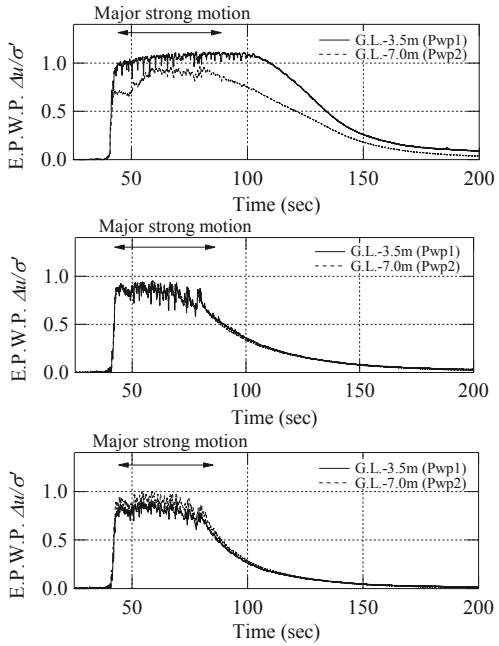


Figure 8. Time histories of excess pore water pressure at Pwp1 and Pwp2: upper; unimprovement case (B1), middle; fixed-type improvement case (B2), floating-type improvement case (B4)

was not fully liquefied although the excess pore water pressure was generated. Similar tendency was observed in B2, the floating-type improvement case, and the ground in B2 was not also liquefied. It followed that the floating-type improvement as well as the fixed-type one took effect, restricting excess pore water pressure in a liquefiable sandy layer.

### 3.3.2 *Ground settlement*

Figure 9 presents the cumulative ground settlement in Series B in a proto-type scale. Each figure represents the settlement at the top of the lattice-shaped mold and the ground surface inside the grid, respectively. The horizontal axis shows the number of stepwise shaking.

The ground settlement of B1, the unimprovement case, reached 0.23 m in Step 2 and increased every step. The final settlement was 0.72 m in Step 6. This large value was due to the liquefaction of ground in every step. In the meanwhile, the settlements of B2, the fixed-type improvement case, were 0.02 m at the top of the mold and 0.06 m at the ground surface. The large settlement could not be found in the successive shaking steps due to no liquefaction.

As for B3 ~ B6, the floating-type improvement cases, the settlements were a little larger than those of B2 in each shaking step. However, the settlements of B3 ~ B6 were much smaller than those of B1, and the improvement effect of the floating-type was confirmed in terms of ground settlement. Especially, the settlement of B1 increased in every step, and ones of B3 ~ B6, meanwhile, did not increase. Therefore, the floating-type as well as the fixed-type was found to be effective against the ground settlement by liquefaction.

## 4 CONCLUSIONS

This paper examined the countermeasure effect of the floating-type and lattice-shaped cement treatment method by using the numerical analyses and the centrifuge model tests. The main mechanism of this method as a liquefaction countermeasure was that the floating-type treated soil reduced the shear stress that was generated in the stratum between treated soil and unliquefiable stratum. This effectiveness was confirmed by the one-dimensional numerical analyses. The centrifuge model tests resulted that the synchronism of the floating-type treated soil

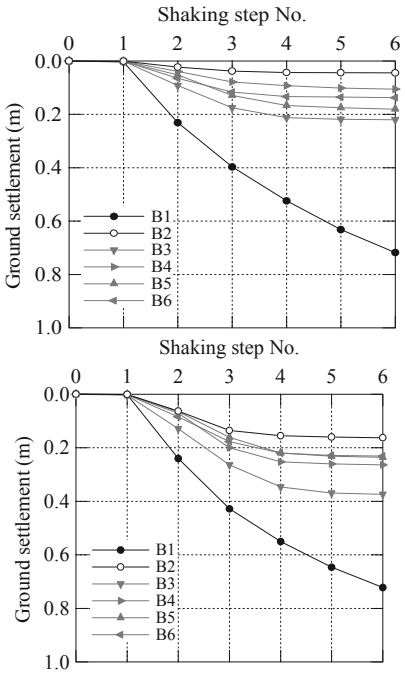


Figure 9. Cumulative ground settlement: upper; top of lattice-shaped mold at Dp1, lower; top of ground surface inside grid at Dp2

and the unliquefiable stratum could restrict the generation of excess pore water pressure the in-between stratum as well as the unimproved soil inside the girds. In addition, the floating-type improvement was found to decrease the ground settlement, and the improvement effect became larger by deepening the depth of the floating-type treated soil.

## ACKNOWLEDGEMENTS

A part of this research was conducted within the collaborative project of Port and Airport Research Institute, Penta Ocean Construction Co., Shimizu Co., Takenaka Civil Engineering & Construction Co., Toa Co., Toyo Co., and Fudo Tetra Co. The authors are very grateful for their valuable cooperation in our work.

## REFERENCES

Kitazume M. and Miyajima S. 1995. Development of PHRI Mark II geotechnical centrifuge. *Technical Note of the Port and Harbour Research Institute* (817), 1-33.

Okamura M. and Inoue T. 2012. Preparation of fully saturated models for liquefaction study. *International Journal of Physical Modelling in Geotechnics* 12(1), 39-46.

Takahashi H., Kitazume M. and Ishibashi S. 2006a. Effect of deep mixing wall spacing on liquefaction mitigation. *Proceedings of the International Conference on Physical Modelling in Geotechnics* 1, 585-590.

Takahashi H., Kitazume M., Ishibashi S. and Yamawaki S. 2006b. Evaluating the saturation of model ground by P-wave velocity and modeling of models for a liquefaction study. *International Journal of Physical Modelling in Geotechnics* 6(1), 13-25.

Takahashi H., Yamawaki S., Kitazume M. and Ishibashi S. 2006c. Effects of deep mixing method on liquefaction prevention and proposal on new arrangement of grid-type improvement. *Report of the Port and Airport Research Institute* 45(2), 135-167. (in Japanese)